Coupling of finite element and boundary integral methods for electromagnetic scattering in a two-layered medium ☆

Peijun Li

Department of Mathematics, Purdue University, West Lafayette, IN 47907, United States

ABSTRACT

Consider a time-harmonic electromagnetic plane wave incident on an inhomogeneity embedded in a two-layered medium. In this paper, a method of coupling of finite element and boundary integral equation methods is presented for the solutions of electromagnetic scattering in both transverse electric and magnetic polarization cases. The well-posedness of the continuous and discrete problems, as well as optimal error estimates for the coupled variational approximations, are obtained. Numerical results are included to illustrate the accuracy with the optimal convergence property of the proposed method and to show the wave features in a two-layered medium.

Published by Elsevier Inc.

1. Introduction

Consider the system of time-harmonic (time dependence $e^{-i\omega t}$) Maxwell's equations in three dimensions

$$\text{curl}\, \mathbf{E} = i\omega \mathbf{B}, \tag{1.1}$$

$$\text{curl}\, \mathbf{H} = -i\omega \mathbf{D} + \mathbf{J}, \tag{1.2}$$

where $\mathbf{E}$ is the electric field, $\mathbf{H}$ is the magnetic field, $\mathbf{B}$ is the magnetic flux density, $\mathbf{D}$ is the electric flux density, $\mathbf{J}$ is the electric current density, and ω is the angular frequency. The constitutive relations, describing the macroscopic properties of the medium, are taken as

$$\mathbf{B} = \mu \mathbf{H}, \quad \mathbf{D} = \varepsilon \mathbf{E}, \quad \text{and} \quad \mathbf{J} = \sigma \mathbf{E},$$

where the constitutive parameters μ, ε, and σ denote, respectively, the magnetic permeability, the electric permittivity, and the conductivity of the medium. Substituting the constitutive relations into Eqs. (1.1) and (1.2) gives a coupled system for the electric and magnetic fields

$$\operatorname{curl}\mathbf{E} = i\omega\mu\mathbf{H}, \tag{1.3}$$
$$\operatorname{curl}\mathbf{H} = (-i\omega\varepsilon + \sigma)\mathbf{E}. \tag{1.4}$$

The fields are assumed to be nonmagnetic, i.e., $\mu = \mu_0$, where μ_0 is the permeability of the vacuum.

Taking the curl of Eq. (1.3) and eliminating the magnetic field from Eq. (1.4), we obtain the equation for the electric field

$$\operatorname{curl}\operatorname{curl}\mathbf{E} - \kappa^2\mathbf{E} = 0, \tag{1.5}$$

where $\kappa^2 = \omega^2\mu_0\varepsilon + i\omega\mu_0\sigma$ and κ is known as the wavenumber. Similarly, we may derive the equation for the magnetic field by eliminating the electric field

$$\operatorname{curl}\kappa^{-2}\operatorname{curl}\mathbf{H} - \mathbf{H} = 0. \tag{1.6}$$

For the transverse electric (TE) polarization case, the incident wave has the electric field parallel to the x_3-axis, which is also the infinite axis of the aperture. Since both the incident field and medium are uniform along the x_3-axis, i.e., no variation of any kind with respect to x_3, the scattered electric field, and thus the total electric field, are also parallel to the x_3-axis, i.e., $\mathbf{E} = [0, 0, u^{\mathrm{tol}}]^\top$. It is therefore convenient to formulate the problem in terms of the electric field since it has only one component. It deduces from Eq. (1.5) that the total electric field satisfies

$$\Delta u^{\mathrm{tol}} + \kappa^2 u^{\mathrm{tol}} = 0 \quad \text{in } \mathbb{R}^2.$$

For the case of transverse magnetic (TM) polarization, the magnetic field has only a x_3-component, i.e., $\mathbf{H} = [0, 0, u^{\mathrm{tol}}]^\top$, and therefore it is convenient to formulate the problem in terms of the magnetic field. It follows from Eq. (1.6) that the total magnetic field satisfies

$$\nabla \cdot \left(\kappa^{-2}\nabla u^{\mathrm{tol}}\right) + u^{\mathrm{tol}} = 0 \quad \text{in } \mathbb{R}^2.$$

In this paper, we will focus on the problems of solving the electromagnetic scattering from an inhomogeneity which is embedded in a two-layered background medium. The extension of the scattering problem to a multi-layered background medium is straightforward since the analytical forms of the fundamental solution can be similarly obtained for the two-dimensional Helmholtz equation in the multi-layered background medium. Scattering problems in layered medium are of important applications in broad scientific areas such as submarine detection, geophysical exploration, near-field optical microscopy, and near-field optics modeling [6,15,33]. Near-field optics has developed dramatically in recent years as an effective approach to breaking the diffraction limit and obtaining images with subwavelength resolution [16], which leads to various applications in biology, chemistry, material sciences, and information storage. We restrict our attention to the scalar cases in two dimensions for simplicity. The more complicated three-dimensional problem will be considered in a separate work.

Consider an experiment where an inhomogeneous sample is embedded in a two-layered medium, either in the upper-half space or in the lower-half space. Excluding the domain of the sample, the wavenumber is assumed to be κ_1 in the upper-half space and κ_2 in the lower-half space, as seen in Fig. 1. To clarify the role of the background medium, the wavenumber is written as $\kappa^2 = \kappa_{\mathrm{b}}^2\varepsilon_{\mathrm{r}}$, where the background wavenumber

$$\kappa_{\mathrm{b}} = \begin{cases} \kappa_1 & \text{for } x_2 > 0, \\ \kappa_2 & \text{for } x_2 < 0, \end{cases}$$

and the relative permittivity ε_{r} varies within the domain of the sample but otherwise has a value of unit.

To apply numerical methods, the open domain needs to be truncated into a bounded domain. Therefore, a suitable boundary condition then has to be imposed on the boundary of the bounded domain so that no artificial wave reflection occurs.
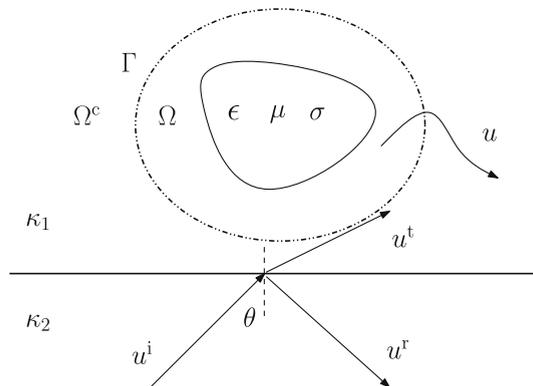
Fig. 1. Problem geometry.

There are a variety of ways to provide such a "non-reflecting" boundary condition, e.g. nonlocal Dirichlet-to-Neumann maps (e.g. [5,25,41]); local absorbing boundary conditions as approximations to nonlocal Dirichlet-to-Neumann maps (e.g. [21,26,27]); perfectly matched layer techniques (e.g. [7,40]); and boundary integral equations (e.g. [31]). It depends on specific problems to choose appropriate boundary conditions mentioned above. However, much effort is currently devoted to the case of a homogeneous background medium and the development of boundary conditions for a layered background medium is still on-going.

Here I present a method of coupling of a boundary integral method for the truncated domain combined with a finite element method in the nonhomogeneous sample. Essentially, the boundary integral equation provides a transparent boundary condition on the boundary of the truncated domain. In this method, the unbounded region was first divided into an interior region and an exterior region. The field in the interior region was formulated using the finite element method, and the field in the exterior region was formulated via the boundary integral method. The interior and exterior fields were subsequently coupled by the continuity conditions at the boundary separating the two regions. This technique is particularly attractive for open-region problems involving complex structures and inhomogeneous materials (e.g. [1–4,9,14,23,24,28,30,35,43]). We refer to Xu [42] for the generalized radiation condition for scattering in stratified medium, to Cutzach and Hazard [18] for the well-posedness and analyticity properties of electromagnetic fields in a two-layered background medium. See also Chandler-Wilde and Zhang [10], Coyle [17], Durán et al. [19], and Zhang and Chandler-Wilde [44] for related scattering problems in a layered medium or in half-space geometry. One may consult Colton and Kress [12,13], Nédélec [37], and Monk [36] for recent accounts of the integral equation methods and finite element methods for acoustic and electromagnetic scattering problems.

The outline of this paper is as follows. Section 2 is devoted to the TE polarization case. A mathematical model is described; variational formulations for coupling a finite element method in the inhomogeneous sample with a boundary integral method on the artificial boundary is presented; the well-posedness of the continuous and discrete problems, as well as optimal error estimates for the coupled variational approximation, are obtained. Parallel results for the case of TM polarization are given in Section 3. In Sections 4 and 5 we discuss the numerical techniques and implementation of the coupling method, and present several numerical experiments to illustrate the accuracy with the optimal convergence property of the proposed method and to show the wave patterns in a two-layered background medium. The paper is concluded with some general remarks and directions for future research in Section 6.

2. TE polarization

In this section, we shall introduce a mathematical model and variational formulation for the scattering problem using the coupling of finite element and boundary integral methods. As the discussion for the TE polarization and TM polarization are parallel, we shall concentrate on the TE polarization first, and state the corresponding results on the TM polarization without proofs.

2.1. Model problem

Throughout, to specify the problem geometry, we assume the sample lies in the upper-half space and the incident wave comes from the lower-half space. As for other problem geometries, the results will be same by just switching the values of the background wavenumber κ_1 and κ_2, and taking a different incident angle.

Let an incoming plane wave $u^i = \exp(i\alpha x_1 + i\beta x_2)$ be incident on the straight line $\{x_2 = 0\}$ from below $\mathbb{R}^2_- = \{\mathbf{x} : x_2 < 0\}$, where $\alpha = \kappa_2 \sin\theta$, $\beta = \kappa_2 \cos\theta$, $\theta \in (-\pi/2, \pi/2)$ is the angle of incidence. By assuming nonmagnetic materials and transverse electric polarization, the model equation reduces to

$$\Delta u^{\text{tol}} + \kappa^2 u^{\text{tol}} = 0 \quad \text{in } \mathbb{R}^2. \tag{2.1}$$

Denote the reference field u^{ref} as the solution of the homogeneous equation:

$$\Delta u^{\text{ref}} + \kappa_b^2 u^{\text{ref}} = 0 \quad \text{in } \mathbb{R}^2. \tag{2.2}$$

It can be shown from the continuity conditions

$$\begin{cases} u^{\text{ref}}(\mathbf{x})|_{x_2=0^+} = u^{\text{ref}}(\mathbf{x})|_{x_2=0^-}, \\ \frac{\partial u^{\text{ref}}(\mathbf{x})}{\partial x_2}\Big|_{x_2=0^+} = \frac{\partial u^{\text{ref}}(\mathbf{x})}{\partial x_2}\Big|_{x_2=0^-} \end{cases}$$

that

$$u^{\text{ref}} = \begin{cases} u^t & \text{for } x_2 > 0, \\ u^i + u^r & \text{for } x_2 < 0, \end{cases}$$

where u^t and u^r are the transmitted and reflected waves, respectively. Precisely, we have

$$u^t = t\exp(i\alpha x_1 + i\gamma x_2) \quad \text{and} \quad u^r = r\exp(i\alpha x_1 - i\beta x_2), \tag{2.3}$$

where the transmission coefficient $t = 2\beta/(\beta + \gamma)$, the reflection coefficient $r = (\beta - \gamma)/(\beta + \gamma)$, and

$$\gamma(\alpha) = \begin{cases} \sqrt{\kappa_1^2 - \alpha^2} & \text{for } \kappa_1 > |\alpha|, \\ i\sqrt{\alpha^2 - \kappa_1^2} & \text{for } \kappa_1 < |\alpha|. \end{cases}$$

The total field u^{tol} consists of the reference field u^{ref} and the scattered field u:

$$u^{\text{tol}} = u^{\text{ref}} + u. \tag{2.4}$$

It follows from Eqs. (2.1), (2.2) and (2.4) that the scattered field satisfies

$$\Delta u + \kappa^2 u = -f \quad \text{in } \mathbb{R}^2, \tag{2.5}$$

where $f = \kappa_b^2(\varepsilon_r - 1)u^{\text{ref}}$ and has a compact support. In addition, the scattered field is required to satisfy the following radiation condition

$$\frac{\partial u}{\partial \rho} - i\kappa_b u = o(\rho^{-1/2}) \tag{2.6}$$

uniformly in all angles as $\rho = |\mathbf{x}| \to \infty$.

We shall use the following notations: for a bounded region Ω in $\mathbb{R}^2$ with boundary Γ, $H^s(\Omega)$ and $H^s(\Gamma)$ will denote the usual Sobolev spaces with norm $\|\cdot\|_{s,\Omega}$ and $\|\cdot\|_{s,\Gamma}$, respectively. To simplify the proofs, we shall employ a positive constant C as a generic constant whose precise value is not required and may change line by line, but should always be clear from the context.

2.2. Variational formulation

Let Ω, containing the compact support of the scatterer, be a smooth bounded domain with boundary Γ, and let $\Omega^c = \mathbb{R}^2 \setminus \overline{\Omega}$ be the complementary set of Ω, as shown in Fig. 1. In the following, a variational formulation for the scattering problem will be derived by using the coupling of the finite element and boundary integral methods, and useful properties of potential operators will be described.

The problem (2.5) and (2.6) can be formulated as the transmission problem

$$\begin{cases} \Delta u_1 + \kappa^2 u_1 = -f & \text{in } \Omega, \\ \Delta u_2 + \kappa_b^2 u_2 = 0 & \text{in } \Omega^c, \\ \gamma_0^- u_1 = \gamma_0^+ u_2 & \text{on } \Gamma, \\ \gamma_1^- u_1 = \gamma_1^+ u_2 = \phi & \text{on } \Gamma, \\ \frac{\partial u_2}{\partial \rho} - i\kappa_b u_2 = o(\rho^{-1/2}) & \text{as } \rho \to \infty. \end{cases} \tag{2.7}$$

Here ϕ is the normal derivative of the field on the boundary Γ and $\gamma_0^- : H^1(\Omega) \to H^{1/2}(\Gamma)$ is the trace operator defined by

$$\gamma_0^- u(\mathbf{x}) := \lim_{\Omega \ni \mathbf{y} \to \mathbf{x}} u(\mathbf{y}) \quad \text{for } \mathbf{x} \in \Gamma,$$

whereas γ_1^- is the associated conormal derivative

$$\gamma_1^- u(\mathbf{x}) := \lim_{\Omega \ni \mathbf{y} \to \mathbf{x}} \left[\mathbf{n_x} \cdot \nabla_{\mathbf{y}} u(\mathbf{y}) \right] \quad \text{for } \mathbf{x} \in \Gamma,$$

where $\mathbf{n_x}$ is the outer normal vector defined for almost all $\mathbf{x} \in \Gamma$. The trace operators γ_0^+ and γ_1^+ are similarly defined in terms of the domain Ω^c.

Let $(\cdot, \cdot)$ denote the duality between $H^1(\Omega)$ and $H^{-1}(\Omega)$, the dual space of $H^1(\Omega)$, with

$$(u, v) = \int_\Omega u \overline{v} d\mathbf{x},$$

and $\langle \cdot, \cdot \rangle$ denote the duality between $H^{1/2}(\Gamma)$ and $H^{-1/2}(\Gamma)$, the dual space of $H^{1/2}(\Gamma)$, with

$$\langle \phi, \psi \rangle = \int_\Gamma \phi \overline{\psi} ds,$$

where the overbar is the complex conjugate.

In Ω, the problem (2.7) has a variational form: find $u \in H^1(\Omega)$ such that

$$a_{\text{TE}}(u_1, v) - \langle \gamma_1^- u_1, \gamma_0^- v \rangle = (f, v) \quad \text{for all } v \in H^1(\Omega), \tag{2.8}$$

where the bilinear form is defined by

$$a_{\mathrm{TE}}(u, v) = \int_{\Omega} (\nabla u \cdot \nabla \overline{v} - \kappa^2 u \overline{v}) d\mathbf{x}.$$

Regarding Ω^c, based on the radiation condition, it follows from Green's theorem and jump relations for surface potentials that the scattered field satisfies the integral equation:

$$\frac{1}{2} (\gamma_0^+ u_2)(\mathbf{x}) = \int_{\Gamma} \frac{\partial G_{\mathrm{TE}}(\mathbf{x}, \mathbf{y})}{\partial \mathbf{n_y}} (\gamma_0^+ u_2)(\mathbf{y}) ds_{\mathbf{y}} - \int_{\Gamma} G_{\mathrm{TE}}(\mathbf{x}, \mathbf{y})(\gamma_1^+ u_2)(\mathbf{y}) ds_{\mathbf{y}} \quad \mathbf{x} \in \Gamma, \tag{2.9}$$

where $G_{\mathrm{TE}}(\mathbf{x}, \mathbf{y}) = \Phi_{\mathrm{TE}}(\mathbf{x}, \mathbf{y}) + \Psi_{\mathrm{TE}}(\mathbf{x}, \mathbf{y})$ is the fundamental solution for the Helmholtz equation in a two-layered background medium, given in the Appendix. The function Φ_{TE} is the fundamental solution of the Helmholtz equation in homogeneous medium and Ψ_{TE} is an infinitely smooth function accounting for the reflections due to the layered medium.

For the study of the boundary integral Eq. (2.9), we introduce two single-layer potential operators

$$\left(V_{\mathrm{TE}}^{(1)} \phi \right)(\mathbf{x}) = 2 \int_{\Gamma} \Phi_{\mathrm{TE}}(\mathbf{x}, \mathbf{y}) \phi(\mathbf{y}) ds_{\mathbf{y}},$$

$$\left(V_{\mathrm{TE}}^{(2)} \phi \right)(\mathbf{x}) = 2 \int_{\Gamma} \Psi_{\mathrm{TE}}(\mathbf{x}, \mathbf{y}) \phi(\mathbf{y}) ds_{\mathbf{y}},$$

and a double-layer potential operator

$$(K_{\mathrm{TE}} \psi)(\mathbf{x}) = 2 \int_{\Gamma} \frac{\partial G_{\mathrm{TE}}(\mathbf{x}, \mathbf{y})}{\partial \mathbf{n_y}} \psi(\mathbf{y}) ds_{\mathbf{y}}.$$

Using these operators, Eq. (2.9) can be written as

$$\gamma_0^+ u_2 - K_{\mathrm{TE}}(\gamma_0^+ u_2) + V_{\mathrm{TE}}(\gamma_1^+ u_2) = 0, \tag{2.10}$$

where $V_{\mathrm{TE}} = V_{\mathrm{TE}}^{(1)} + V_{\mathrm{TE}}^{(2)}$ is also a single-layer potential operator.

Lemma 2.1. *The single-layer potential operators $V_{\mathrm{TE}}^{(1)}$, $V_{\mathrm{TE}}^{(2)}$, and V_{TE} are compact from $H^{-1/2}(\Gamma)$ into $H^{1/2}(\Gamma)$, and the double-layer potential operator K_{TE} is compact from $H^{1/2}(\Gamma)$ into $H^{1/2}(\Gamma)$.*

Proof. It follows from the Appendix that the function Ψ_{TE} is infinitely smooth and therefore the operator $V_{\mathrm{TE}}^{(2)}$ and K_{TE} are compact (Theorem 2.6, Colton and Kress [12]). Since Φ_{TE} is the fundamental solution of the Helmholtz equation in homogeneous background, the potential operator $V_{\mathrm{TE}}^{(1)}$ is compact (Theorem 3.4.1 [37]). □

We recall the following useful result (Theorem 7.6 [34]) for the coercivity property of the operator $V_{\mathrm{TE}}^{(1)}$:

Lemma 2.2. *There exists a positive constant C such that*

$$\mathrm{Re}\left[(1 - i) \left\langle V_{\mathrm{TE}}^{(1)} \phi, \phi \right\rangle \right] \geqslant C \|\phi\|_{-1/2,\Gamma}^2 \quad \text{for all } \phi \in H^{-1/2}(\Gamma).$$

Multiplying Eq. (2.10) by the complex conjugate of ψ and integrating over Γ, it follows that

$$\langle \gamma_0^+ u_2, \psi \rangle - \langle K_{\mathrm{TE}}(\gamma_0^+ u_2), \psi \rangle + \langle V_{\mathrm{TE}}(\gamma_1^+ u_2), \phi \rangle = 0 \quad \text{for all } \psi \in H^{-1/2}(\Gamma).$$

Using the continuity conditions, we arrive at the following problem: find $[u, \phi] \in H^1(\Omega) \times H^{-1/2}(\Gamma)$ such that

$$\begin{cases} a_{\mathrm{TE}}(u, v) - \langle \phi, v \rangle = (f, v) & \text{for all } v \in H^1(\Omega) \\ \langle u, \psi \rangle - \langle K_{\mathrm{TE}} u, \psi \rangle + \langle V_{\mathrm{TE}} \phi, \psi \rangle = 0 & \text{for all } \psi \in H^{-1/2}(\Gamma) \end{cases}, \tag{2.11}$$

which consist of the variational formulation for the coupling of the finite element and boundary integral methods.

2.3. Uniqueness and existence

We first give a simple proof of the uniqueness for the equivalent transmission problem (2.7) for loss medium, i.e., $\sigma > 0$, and then establish the existence of solution for the variational formulation since our numerical method is based on variational formulation.

Lemma 2.3. *The problem (2.5) and (2.6) has at most one solution.*

Proof. It suffices to show that $u = 0$ if $f = 0$. Let B_ρ, containing the compact support of the scatterer, be a disc with radius ρ and boundary S_ρ. We have from the radiation condition that

$$\left| \frac{\partial u}{\partial \rho} - i\kappa_b u \right|^2 = \left| \frac{\partial u}{\partial \rho} \right|^2 + \kappa_b^2 |u|^2 + 2\kappa_b \, \mathrm{Im}\left(\frac{\partial \overline{u}}{\partial \mathbf{n}} u \right) = o(\rho) \quad \text{as } \rho \to \infty. \tag{2.12}$$

Multiplying the complex conjugate of u and integrating by parts for Eq. (2.5), it follows from the Green's theorem that

$$\int_{B_\rho} \left(|\nabla u|^2 - \bar{\kappa}^2 |u|^2\right) d\mathbf{x} = \int_{S_\rho} \frac{\partial \overline{u}}{\partial \mathbf{n}} u \, ds,$$

which yields

$$\mathrm{Im} \int_{S_\rho} \frac{\partial \overline{u}}{\partial \mathbf{n}} u \, ds = \omega \mu_0 \int_{B_\rho} \sigma |u|^2 d\mathbf{x}. \tag{2.13}$$

Combining Eqs. (2.12) and (2.13) give

$$\int_{S_\rho} \left(\kappa_b^{-1} \left|\frac{\partial u}{\partial \rho}\right|^2 + \kappa_b |u|^2 \right) ds + 2\omega\mu_0 \int_{B_\rho} \sigma |u|^2 d\mathbf{x} \to 0 \quad \text{as } \rho \to \infty.$$

Hence u must be identically zero in $\mathbb{R}^2$. $\square$

Remark 2.1. Lemma 2.3 is an extension of the result of Rellich (Lemma 2.11 [12]) to the case of a two-layered background medium. We refer to Kristensson [32] for a sophisticated uniqueness proof for more general continuity conditions and geometry in the lossless case, i.e., $\sigma = 0$.

Introduce two operators $A_1, A_2 : H^1(\Omega) \to H^{-1}(\Omega)$ given by

$$(A_1 u, v)_1 = (\nabla u, \nabla v) + (\kappa^2 u, v), \tag{2.14}$$
$$(A_2 u, v)_1 = 2(\kappa^2 u, v), \tag{2.15}$$

where $(\cdot, \cdot)_1$ defines a duality between $H^1(\Omega)$ and $H^{-1}(\Omega)$. With these operators, we construct the operator

$$\mathbf{A} : H^1(\Omega) \times H^{-1/2}(\Gamma) \to H^{-1}(\Omega) \times H^{1/2}(\Gamma)$$

given by

$$\mathbf{A} = \begin{bmatrix} A_1 - A_2 & -I \\ I - K_{\mathrm{TE}} & V_{\mathrm{TE}}^{(1)} + V_{\mathrm{TE}}^{(2)} \end{bmatrix}.$$

Denote $\mathcal{V} = H^1(\Omega) \times H^{-1/2}(\Gamma)$, then for any $\mathbf{u} = [u, \phi]$, $\mathbf{v} = [v, \psi] \in \mathcal{V}$, we define a duality between $\mathcal{V}$ and $\mathcal{V}'$, the dual of $\mathcal{V}$:

$$\{\mathbf{A}\mathbf{u}, \mathbf{v}\} = (A_1 u, v)_1 - (A_2 u, v)_1 - \langle \phi, v \rangle + \langle u, \psi \rangle - \langle K_{\mathrm{TE}} u, \psi \rangle + \left\langle V_{\mathrm{TE}}^{(1)} \phi, \psi \right\rangle + \left\langle V_{\mathrm{TE}}^{(2)} \phi, \psi \right\rangle.$$

The variational problem (2.11) can be formulated as: find $\mathbf{u} = [u, \phi]$, such that

$$\{\mathbf{A}\mathbf{u}, \mathbf{v}\} = \{\mathbf{f}, \mathbf{v}\}_{\mathcal{V}} \quad \text{for all } \mathbf{v} \in \mathcal{V}. \tag{2.16}$$

Here $\{\cdot, \cdot\}_{\mathcal{V}}$ denotes the scalar product in $\mathcal{V}' \times \mathcal{V}$ and $\mathbf{f} = [-f, 0]$. The norm in $\mathcal{V}$ is naturally defined as

$$\|\mathbf{u}\|_{\mathcal{V}} = \left(\|u\|_{1,\Omega}^2 + \|\phi\|_{-1/2,\Gamma}^2\right)^{1/2}. \tag{2.17}$$

Theorem 2.1. *The operator $\mathbf{A}$ is Fredholm of index zero.*

Proof. Decompose the operator $\mathbf{A} = \mathbf{A}_1 + \mathbf{A}_2$, where

$$\mathbf{A}_1 = \begin{bmatrix} A_1 & -I \\ I & V_{\mathrm{TE}}^{(1)} \end{bmatrix} \quad \text{and} \quad \mathbf{A}_2 = \begin{bmatrix} -A_2 & 0 \\ -K_{\mathrm{TE}} & V_{\mathrm{TE}}^{(2)} \end{bmatrix}.$$

Evidently, A_2 is compact from (2.15) and thus $\mathbf{A}_2$ is compact. It suffices check the coercivity of $\mathbf{A}_1$. For any $\mathbf{u} \in \mathcal{V}$,

$$\{\mathbf{A}_1 \mathbf{u}, \mathbf{u}\} = (\nabla u, \nabla u) + (\kappa^2 u, u) - \langle \phi, u \rangle + \langle u, \phi \rangle + \langle V_1 \phi, \phi \rangle.$$

It follows from Lemma 2.2 that

$$|\{\mathbf{A}_1 \mathbf{u}, \mathbf{u}\}| \geqslant C_1 \|u\|_{1,\Omega}^2 + C_2 \|\phi\|_{-1/2,\Gamma}^2 \geqslant C \|\mathbf{u}\|_{\mathcal{V}}^2.$$

Therefore $\mathbf{A}_1$ is invertible and $\mathbf{A} = \mathbf{A}_1 + \mathbf{A}_2$ is Fredholm of index zero (Theorem 2.33 [34]). $\square$

The existence of the solution for variational formulation (2.11) immediately follows from the Fredholm alternative (Theorem 2.27 [34]).

Theorem 2.2. *Given the relative permittivity $\varepsilon_r \in L^\infty(\Omega)$, the variational problem (2.11) admits a unique solution $[u, \phi] \in \mathcal{V}$.*

Remark 2.2. It was proved in Theorem 2.2 that there exists a unique solution $u \in H^1(\Omega)$. Elliptic regularity theory implies that $u \in H^2(\Omega)$. However, one can not expect better regularity for u when $\varepsilon_r \in L^\infty(\Omega)$ as in Theorem 2.2.

2.4. The discrete problem

In this section, the well-posedness of the discrete problem and optimal error estimates for the coupled variational approximation are studied. Let $\mathbf{x}(t)$ be a parametrization of the boundary Γ, where $0 \leqslant t \leqslant 1$. Given any parameter $h \in (0,1]$, let $0 = t_0 \leqslant t_1 \leqslant \cdots \leqslant t_N = 1$ be a partition of $[0,1]$ with $t_{i+1} - t_i = h_i < h$ for $i = 0, \ldots, N-1$. We denote by Ω_h the polygonal domain that approximates Ω with vertices on the boundary Γ are $\{\mathbf{x}(t_i), i = 1, \ldots, N\}$. Let $\tilde{\mathcal{J}}_h$ be a regular triangulation of $\bar{\Omega}_h$ by triangles $\tilde{T}$ with diameter $h_{\tilde{T}}$ no greater than h. We thus obtain from $\tilde{\mathcal{J}}_h$ a triangulation $\mathcal{J}_h$ of $\bar{\Omega}$, replacing each triangle $\tilde{T} \in \tilde{\mathcal{J}}_h$ with one side along a curved part of Γ by the corresponding curved triangle T, which leads to $\Omega = \cup_{T \in \mathcal{J}_h} T$.

Define conforming finite element subspaces X_h of $H^1(\Omega)$ and Y_h of $H^{-1/2}(\Gamma)$, and consider the discrete problem: find $[u_h, \phi_h] \in X_h \times Y_h$ such that

$$\begin{cases} a_{\mathrm{TE}}(u_h, v) - \langle \phi_h, v \rangle = (f, v) & \text{for all } v \in X_h, \\ \langle u_h, \psi \rangle - \langle K_{\mathrm{TE}} u_h, \psi \rangle + \langle V_{\mathrm{TE}} \phi_h, \psi \rangle = 0, & \text{for all } \psi \in Y_h. \end{cases} \tag{2.18}$$

Let $\mathcal{V}_h = X_h \times Y_h$ and the variational form of the discrete problem is equivalent to: find $\mathbf{u}_h = [u_h, \phi_h] \in \mathcal{V}_h$ such that

$$\{\mathbf{A}\mathbf{u}_h, \mathbf{v}\} = \{\mathbf{f}, \mathbf{v}\}_\mathcal{V} \quad \text{for all } \mathbf{v} \in \mathcal{V}_h. \tag{2.19}$$

We shall now prove that for h small enough the discrete problem (2.19) admits a unique solution $\mathbf{u}_h \in \mathcal{V}_\langle$ and then provide an optimal estimate of the error.

Theorem 2.3. Let $\mathbf{u} = [u, \phi] \in \mathcal{V}$ be the solution of the continuous problem (2.16). For sufficiently small h, the discrete problem (2.19) has a unique solution $\mathbf{u_h} = [u_h, \phi_h] \in \mathcal{V}_h$ that satisfies

$$\|u - u_h\|_{1,\Omega} + \|\phi - \phi_h\|_{-1/2,\Gamma} \leqslant C \left(\inf_{v \in X_h} \|u - v\|_{1,\Gamma} + \inf_{\psi \in Y_h} \|\phi - \psi\|_{-1/2,\Gamma} \right). \tag{2.20}$$

Proof. It follows from the uniqueness of the solution of (2.16) that the operator $\mathbf{A}$ is one-to-one. Thus, it is also onto, and the open mapping theorem proves that $\mathbf{A}^{-1} : \mathcal{V}' \to \mathcal{V}$ is continuous. Therefore, $\mathbf{A} = \mathbf{A}_1 + \mathbf{A}_2$ is an isomorphism, $\mathbf{A}_1$ is coercive, and $\mathbf{A}_2$ is compact. An application of Theorem 10.1.2 in Chen and Zhou [11] yields that there exists an $h_0 > 0$ and some constant C independent of h with $h < h_0$ such that

$$\sup_{\mathbf{u} \in \mathcal{V}_h, \|\mathbf{u}\|_\mathcal{V}=1} \{\mathbf{A}\mathbf{u}, \mathbf{v}\} \geqslant C\|\mathbf{v}\|_\mathcal{V}. \tag{2.21}$$

Since the adjoint operators $\mathbf{A}^*$, $\mathbf{A}_1^*$, and $\mathbf{A}_2^*$ have the same properties as $\mathbf{A}$, $\mathbf{A}_1$, and $\mathbf{A}_2$, we also have for sufficiently small h that

$$\sup_{\mathbf{v} \in \mathcal{V}_h, \|\mathbf{v}\|_\mathcal{V}=1} \{\mathbf{A}\mathbf{u}, \mathbf{v}\} \geqslant C\|\mathbf{u}\|_\mathcal{V} \tag{2.22}$$

for some C. It follows from the above Babuška coercivity conditions (2.21) and (2.22) that the discrete variational problem (2.19) has a unique solution $\mathbf{u}_h = [u_h, \phi_h] \in \mathcal{V}_h$ satisfying

$$\|\mathbf{u} - \mathbf{u}_h\|_\mathcal{V} \leqslant C \inf_{\mathbf{v} \in \mathcal{V}_h} \|\mathbf{u} - \mathbf{v}\|_\mathcal{V}$$

for all sufficiently small h. The proof is complete by a simple application of the Scharwz inequality and the definition of the norm in $\mathcal{V}$ from Eq. (2.17). $\square$

Remark 2.3. If the finite element spaces X_h and Y_h have the approximation properties

$$\|u - \Pi_\Omega u\|_{1,\Omega} \leqslant Ch^s \|u\|_{s+1,\Omega}, \quad 0 < s \leqslant m-1,$$
$$\|\phi - \Pi_\Gamma \phi\|_{-1/2,\Gamma} \leqslant Ch^s \|\phi\|_{s-1/2,\Gamma}, \quad 0 < s \leqslant m-1,$$

where $\Pi_\Omega : H^m(\Omega) \to X_h$ and $\Pi_\Gamma : H^{m-1/2}(\Gamma) \to Y_h$ are interpolation operators, we can obtain the following error estimate

$$\|u - u_h\|_{1,\Omega} + \|\phi - \phi_h\|_{-1/2,\Gamma} \leqslant Ch^s \left(\|u\|_{s+1,\Omega} + \|\phi\|_{s-1/2,\Gamma} \right).$$

Remark 2.4. Define by X_h the piecewise linear finite element subspace of $H^1(\Omega)$. For a regular triangulation $\mathcal{J}_h$, the usual technique used in the affine case gives rise to interpolation error bounds in terms of order h (e.g. [8]), i.e.,

$$\inf_{v \in X_h} \|u - v\|_1 \leqslant Ch\|u\|_2. \tag{2.23}$$

Let Y_h be the space of piecewise constant functions on the partition: $0 = t_0 \leqslant t_1 \leqslant \cdots \leqslant t_N = 1$. It is known (e.g. [39]) that Y_h is a subspace of $H^{-1/2}(\Omega)$ and satisfies for any $\phi \in H^{1/2}(\Gamma)$

$$\inf_{\psi \in Y_h} \|\phi - \psi\|_{-1/2,\Gamma} \leqslant Ch\|\phi\|_{1/2,\Gamma}. \tag{2.24}$$

3. TM polarization

In this section we state the parallel results for the electromagnetic scattering of an inhomogeneous sample embedded in a layered background medium in the case of transverse magnetic polarization.

Consider the same problem geometry as that in TE polarization case, let an incoming plane wave $u^{\mathrm{i}} = \exp(i\alpha x_1 + i\beta x_2)$ be incident on the straight line $\{x_2 = 0\}$ from $\mathbb{R}^2_- = \mathbf{x} : x_2 < 0\}$, where $\alpha = \kappa_2 \sin\theta$, $\beta = \kappa_2 \cos\theta$, $\theta \in (-\pi/2, \pi/2)$ is the angle of incidence. By assuming nonmagnetic materials and transverse magnetic polarization, the model equation for the total magnetic field is

$$\nabla \cdot \left(\kappa^{-2}\nabla u^{\mathrm{tol}}\right) + u^{\mathrm{tol}} = 0 \quad \text{in } \mathbb{R}^2. \tag{3.1}$$

Denote the reference field u^{ref} as the solution of the homogeneous equation:

$$\nabla \cdot \left(\kappa_b^{-2}\nabla u^{\mathrm{ref}}\right) + u^{\mathrm{ref}} = 0 \quad \text{in } \mathbb{R}^2. \tag{3.2}$$

It can be shown from the continuity conditions

$$u^{\mathrm{ref}}(\mathbf{x})|_{x_2=0^+} = u^{\mathrm{ref}}(\mathbf{x})|_{x_2=0^-},$$

$$\frac{1}{\kappa_1^2}\frac{\partial u^{\mathrm{ref}}(\mathbf{x})}{\partial x_2}\bigg|_{x_2=0^+} = \frac{1}{\kappa_2^2}\frac{\partial u^{\mathrm{ref}}(\mathbf{x})}{\partial x_2}\bigg|_{x_2=0^-}$$

that

$$u^{\mathrm{ref}} = \begin{cases} u^{\mathrm{t}} & \text{for } x_2 > 0, \\ u^{\mathrm{i}} + u^{\mathrm{r}} & \text{for } x_2 < 0, \end{cases}$$

where u^{t} and u^{r} are the transmitted and reflected waves, respectively. Precisely, we have

$$u^{\mathrm{t}} = t\exp(i\alpha x_1 + i\gamma x_2) \quad \text{and} \quad u^{\mathrm{r}} = r\exp(i\alpha x_1 - i\beta x_2), \tag{3.3}$$

where $t = 2\beta\kappa_1^2/(\beta\kappa_1^2 + \gamma\kappa_2^2)$, $r = (\beta\kappa_1^2 - \gamma\kappa_2^2)/(\beta\kappa_1^2 + \gamma\kappa_2^2)$, and

$$\gamma(\alpha) = \begin{cases} \sqrt{\kappa_1^2 - \alpha^2} & \text{for } \kappa_1 > |\alpha|, \\ i\sqrt{\alpha^2 - \kappa_1^2} & \text{for } \kappa_1 < |\alpha|. \end{cases} \tag{3.4}$$

The total field consists of the reference field u^{ref} and the scattered field u:

$$u^{\mathrm{tol}} = u^{\mathrm{ref}} + u. \tag{3.5}$$

It follows from (3.1), (3.2) and (3.5) that the scattered field satisfies.

$$\nabla \cdot \left(\kappa^{-2}\nabla u\right) + u = -g \quad \text{in } \mathbb{R}^2, \tag{3.6}$$

where

$$g = \nabla \cdot \left((\kappa^{-2} - \kappa_b^{-2})\nabla u^{\mathrm{ref}}\right).$$

In addition, the scattered field is required to satisfy the following radiation conditions

$$\frac{\partial u}{\partial \rho} - i\kappa_b u = o(\rho^{-1/2}) \quad \text{as } \rho \to \infty. \tag{3.7}$$

The problem (3.6) and (3.7) can also be formulated as the transmission problem

$$\begin{cases} \nabla \cdot (\kappa^{-2}\nabla u_1) + u_1 = -g & \text{in } \Omega, \\ \nabla \cdot (\kappa_b^{-2}\nabla u_2) + u_2 = 0 & \text{in } \Omega^{\mathrm{c}}, \\ \gamma_0^- u_1 = \gamma_0^+ u_2 & \text{on } \Gamma, \\ \kappa_b^{-2}\gamma_1^- u_1 = \kappa_b^{-2}\gamma_1^+ u_2 = \varphi & \text{on } \Gamma, \\ \frac{\partial u_2}{\partial \rho} - i\kappa_b u_2 = o(\rho^{-1/2}) & \text{as } \rho \to \infty, \end{cases} \tag{3.8}$$

which has an equivalent variational form: find $u \in H^1(\Omega)$ such that

$$a_{\mathrm{TM}}(u, v) - \langle \varphi, v \rangle = (g, v) \quad \text{for all } v \in H^1(\Omega),$$ (3.9)

where the bilinear form is defined by

$$a_{\mathrm{TM}}(u, v) = (\kappa^{-2}\nabla u, \nabla v) - (u, v).$$

To apply potential theory, we introduce a single-layer potential operator $V_{\mathrm{TM}} : H^{-1/2}(\Gamma) \to H^{1/2}(\Gamma)$ and a double-layer potential operator $K_{\mathrm{TM}} : H^{1/2}(\Gamma) \to H^{1/2}(\Gamma)$, which are defined as

$$(V_{\mathrm{TM}}\varphi)(\mathbf{x}) = 2 \int_{\Gamma} G_{\mathrm{TM}}(\mathbf{x}, \mathbf{y})\varphi(\mathbf{y})ds(\mathbf{y}),$$

$$(K_{\mathrm{TM}}\psi)(\mathbf{x}) = 2 \int_{\Gamma} \frac{\partial G_{\mathrm{TM}}(\mathbf{x}, \mathbf{y})}{\partial \mathbf{n}(\mathbf{y})}\psi(\mathbf{y})ds(\mathbf{y}).$$

Here $G_{\mathrm{TM}}(\mathbf{x}, \mathbf{y})$ is the fundamental solution of the Helmholtz equation with a two-layered background medium in $\mathbb{R}^2$ for the TM case, given in Appendix.

Upon using potential operators and continuity conditions, we may obtain the variational formulation for the boundary integral equation

$$\langle u, \psi \rangle - \langle \kappa_{\mathrm{b}}^{-2}K_{\mathrm{TM}}u, \psi \rangle + \langle V_{\mathrm{TM}}\varphi, \psi \rangle = 0 \quad \text{for all } \psi \in H^{-1/2}(\Gamma).$$ (3.10)

Eqs. (3.9) and (3.10) consist of the variational formulation for the coupling of the finite element and boundary integral methods in the case of TM polarization. The following theorems are analogues of Theorems 2.2 and 2.3.

Theorem 3.1. *Given the relative permittivity $\varepsilon_{\mathrm{r}} \in L^{\infty}(\Omega)$, the variational problem (3.9) and (3.10) admits a unique solution $[u, \varphi] \in \mathcal{V}$.*

Theorem 3.2. *Let $\mathbf{u} = [u, \varphi] \in \mathcal{V}$ be the solution of the continuous problem (3.9) and (3.10). For sufficiently small h, the discrete problem to (3.9) and (3.10) has a unique solution $\mathbf{u_h} = [u_h, \varphi_h] \in \mathcal{V}_h$ that satisfies*

$$\|u - u_h\|_{1,\Omega} + \|\varphi - \varphi_h\|_{-1/2,\Gamma} \leqslant C \left(\inf_{v \in X_h} \|u - v\|_{1,\Gamma} + \inf_{\psi \in Y_h} \|\varphi - \psi\|_{-1/2,\Gamma} \right).$$ (3.11)

Remark 3.1. The solution in the TE case is more regular than in the TM case. In general for $\varepsilon_{\mathrm{r}} \in L^{\infty}(\Omega)$, the solution is in $H^2(\Omega)$ in the TE case, while it is in $H^1(\Omega)$ in the TM case. By the result of Elschner and Schmidt [20], the regularity of the solution can be improved to $H^{1+\epsilon}$ for some $\epsilon \in (0, \frac{1}{2})$ in the TM case.

4. Numerical techniques

In this section, we discuss computational aspects of the coupling of finite element and boundary integral equation methods.

4.1. Numerical quadratures

In the implementation of the finite element–boundary integral method, improper and singular integrals have to be evaluated. Two representative examples will be discussed here: one is to apply accurate Gaussian quadratures for evaluating the improper integral (A.3) and the other is to adopt a semi-analytical method for evaluating a singular integral involving the Hankel function.

The improper integral (A.3) can be split into two parts according to the definition of β_1:

$$\int_{-\infty}^{\infty} \frac{1}{\beta_1} \frac{\beta_1 - \beta_2}{\beta_1 + \beta_2} e^{i\beta_1(x_2+y_2)} e^{i\xi(x_1-y_1)} d\xi = \int_{-\kappa_1}^{\kappa_1} \frac{f(\xi)}{\sqrt{\kappa_1^2 - \xi^2}} d\xi - 2i \int_{\kappa_1}^{\infty} \frac{e^{-\sqrt{\xi^2 - \kappa_1^2}(x_2+y_2)}}{\sqrt{\xi^2 - \kappa_1^2}} g(\xi) d\xi$$

where both $f(\xi)$ and $g(\xi)$ are smooth functions, given by

$$f(\xi) = \frac{\beta_1 - \beta_2}{\beta_1 + \beta_2} e^{i\beta_1(x_2+y_2)} e^{i\xi(x_1-y_1)} \quad \text{and} \quad g(\xi) = \frac{\beta_1 - \beta_2}{\beta_1 + \beta_2} \cos(\xi(x_1 - y_1)).$$

Noting the weight function appeared in the integral of the first part, it is natural to consider the Gauss–Chebyshev quadrature which yields

$$\int_{-\kappa_1}^{\kappa} \frac{f(\xi)}{\sqrt{\kappa_1^2 - \xi^2}} d\xi = \int_{-1}^{1} \frac{f(\kappa_1\eta)}{\sqrt{1 - \eta^2}} d\eta \approx \sum_{m=1}^{N_{\mathrm{Ch}}} w_{\mathrm{Ch}}^{(m)} f\left(\kappa_1 \eta_{\mathrm{Ch}}^{(m)}\right),$$

where $\eta_{\mathrm{Ch}}^{(m)}$ and $w_{\mathrm{Le}}^{(m)}$ are the abcissas and weight associated with the Chebyshev polynomial over the interval $[-1, 1]$.

Let $\tau = \sqrt{\xi^2 - \kappa_1^2}$, it follows from the change of variable that the second part can be written as

$$\int_{\kappa_1}^{\infty} \frac{e^{-\sqrt{\xi^2 - \kappa_1^2}(x_2 + y_2)}}{\sqrt{\xi^2 - \kappa_1^2}} g(\xi) d\xi = \int_0^{\infty} e^{-\tau(x_2 + y_2)} h(\tau) d\tau,$$

where $h(\tau)$ is also a smooth function, given as

$$h(\tau) = \frac{\beta_1 - \beta_2}{\beta_1 + \beta_2} \frac{\cos\left(\sqrt{\tau^2 + \kappa_1^2}(x_1 - y_1)\right)}{\sqrt{\tau^2 + \kappa_1^2}}.$$

The Gauss–Laguerre quadrature can thus be used to treat the second part

$$\int_{\kappa_1}^{\infty} \frac{e^{-\sqrt{\xi^2 - \kappa_1^2}(x_2 + y_2)}}{\sqrt{\xi^2 - \kappa_1^2}} g(\xi) d\xi \approx \frac{1}{x_2 + y_2} \sum_{m=1}^{N_{La}} w_{La}^{(m)} h\left(\frac{\tau_{La}^{(m)}}{x_2 + y_2}\right),$$

where $\tau_{La}^{(m)}$ and $w_{La}^{(m)}$ are the abcissas and weight associated with the Laguerre polynomial over the interval $[0, \infty]$.

When the space of piecewise constant functions is used as a finite element subspace to $H^{-1/2}(\Gamma)$, the following integral needs to be evaluated

$$\int_{\Gamma_i} \int_{\Gamma_j} G(\mathbf{x}, \mathbf{y}) ds_{\mathbf{y}} ds_{\mathbf{x}},$$

where Γ_i and Γ_j are two segments of the discretized boundary, and the integrand $G(\mathbf{x}, \mathbf{y})$ represents the fundamental solution. There are two possibilities for the above integral: for $i \neq j$, the integrand is a regular function and Gauss–Legendre quadrature can be used; for $i = j$, a semi-analytical method can be adopted.

If $i \neq j$, we may use the change of variables and convert the line integrals into single integrals. Suppose $\mathbf{x}_1, \mathbf{x}_1$ and $\mathbf{y}_1, \mathbf{y}_2$ are two end points for the line segments Γ_i and Γ_j, respectively. Let $\mathbf{x} = \mathbf{x}_1 + t(\mathbf{x}_2 - \mathbf{x}_1)$, $t \in [0, 1]$ and $\mathbf{y} = \mathbf{y}_1 + s(\mathbf{y}_2 - \mathbf{y}_1)$, $s \in [0, 1]$, we obtain

$$\int_{\Gamma_i} \int_{\Gamma_j} G(\mathbf{x}, \mathbf{y}) ds_{\mathbf{y}} ds_{\mathbf{x}} = |\Gamma_i| |\Gamma_j| \int_0^1 \int_0^1 G(\mathbf{x}(t), \mathbf{y}(s)) ds dt$$

$$\approx |\Gamma_i| |\Gamma_j| \sum_{m,n=1}^{N_{Le}} w_{Le}^{(m)} w_{Le}^{(n)} G(\mathbf{x}(t_{Le}^{(m)}), \mathbf{y}(s_{Le}^{(n)})),$$

where $|\Gamma_i|$ is the length of the segment Γ_i, $t_{Le}^{(m)}$ and $s_{Le}^{(m)}$ are the abcissas, and $w_{Le}^{(m)}$ is the weight associated with the Legendre polynomial over the interval $[0, 1]$.

If $i = j$, the integrand involving the Hankel function becomes singular. However we have the following asymptotic behavior for the fundamental solution to the Helmholtz equation in two dimensions

$$\frac{i}{4} H_0^{(1)}(\kappa_1 |\mathbf{x} - \mathbf{y}|) = -\frac{1}{2\pi} \log(|\mathbf{x} - \mathbf{y}|) + \frac{i}{4} - \frac{\gamma}{2\pi} - \frac{1}{2\pi} \log \frac{\kappa_1}{2} + O\left(|\mathbf{x} - \mathbf{y}|^2 \log(|\mathbf{x} - \mathbf{y}|)\right)$$

as $|\mathbf{x} - \mathbf{y}| \to 0$, where γ is Euler's constant. As can be seen, the fundamental solution to the Helmholtz equation in two dimensions has the same singular behavior as the fundamental solution of Laplace's equation, which can be analytically evaluated

$$\int_{\Gamma_i} \int_{\Gamma_i} \log(|\mathbf{x} - \mathbf{y}|) ds_{\mathbf{y}} ds_{\mathbf{x}} = |\Gamma_i|^2 \left(\log |\Gamma_i| - \frac{3}{2}\right).$$

4.2. Solution techniques

We discuss some solution techniques for the system of equations obtained using the coupling of finite element and boundary integral formulation. The finite element–boundary integral system consists of two set of equations: one results from the finite element discretization which can be written as

$$[A_{11}][u] + [A_{12}][\phi] = [b] \tag{4.1}$$

and the other results from the boundary integral discretization, which can be written as

$$[A_{21}][u] + [A_{22}][\phi] = 0. \tag{4.2}$$

The matrices and vectors appearing in these two equations are described as follows: $[A_{11}]$ is an $N_n \times N_n$ square, symmetric, sparse, and banded matrix; $[A_{12}]$ is an $N_n \times N_e$ rectangular and sparse matrix; $[A_{21}]$ is an $N_e \times N_n$ rectangular and sparse matrix; $[A_{22}]$ is an $N_e \times N_e$ square and fully populated matrix; $[u]$ and $[\phi]$ are N_n and N_e unknown vectors, respectively; $[b]$ is a known N_n vector. Here N_n denotes the total number of unknowns (nodes) in the entire solution domain and N_e is the total

number of unknowns (boundary edges) on the truncation boundary. Usually, the number of nodes N_n is much larger than the number of boundary edges N_e.

The direct approach to solving (4.1) and (4.2) is to solving for u and ϕ simultaneously, i.e., to solve an $(N_n + N_e) \times (N_n + N_e)$ matrix system. This is, however, not efficient since the system involves both sparse and full submatrices, and it is difficult to exploit the symmetry and sparseness of the submatrices A_{11} and A_{12}. I employed the commonly used outward-looking approach, which is composed of two steps. First invert A_{22} and write ϕ in terms of u:

$$[\phi] = -[A_{22}^{-1} A_{21}][u]. \tag{4.3}$$

When this is substituted into the first equation of (4.1) we have

$$\left[A_{11} - A_{12} A_{22}^{-1} A_{21}\right][u] = [b]. \tag{4.4}$$

In this approach, two matrices have to be solved: one is the complex and full matrix A_{22} of size $N_e \times N_e$ and the other is the sparse complex matrix $A_{11} - A_{12} A_{22}^{-1} A_{21}$ of size $N_n \times N_n$. Therefore, the boundary integral system (4.2) is imposed on the finite element system (4.1) as a boundary constraint, which numerically provides a transparent boundary condition. The first matrix is handled once by LU decomposition with partial pivoting. The sparse linear system for (4.4) can be most efficiently solved if the zero elements of the coefficient matrix are not stored. The compressed row storage format is used and all matrices are stored in one-dimensional arrays, which makes no assumptions about the sparsity structure of the matrix and does not store any unnecessary elements. Regarding the linear solver in the second step, the non-symmetric quasi-minimal residual algorithm of Freund and Nachtigal [22] with the diagonal preconditioning is used to solve the sparse and complex system of the equations.

5. Numerical experiments

We report computational results for a set of test problems. In our experiments, the parameters are chosen as follows: $\kappa_1 = 2\pi$, $\kappa_2 = 4\pi$, and the computational domain is a disc with radius 0.75 and center at $(0, 1)$. The piecewise linear and the piecewise constant finite element spaces are used to approximate the field and its normal derivative, respectively. A simple MATLAB mesh generator distmesh2d by Persson and Strang [38] is adopted to generate an approximately uniform mesh. The mesh generator is based on one user-defined function and one user-specified parameter. The function d defines the domain by giving the signed distance from any point (x_1, x_2) to the boundary so that the boundary is defined by $d(x_1, x_2) = 0$. The input parameter h gives the initial edge length for triangles. The code was written in FORTRAN90 using double precision arithmetic and computations were run on an 2.8 GHz Intel Pentium dual quad Xeon processors with 8GB memory.

Example 1 (*TE case*). Consider an incoming plane wave incident normally, i.e., $\theta = 0$, from the lower-half space to the upper-half space, where there is no sample. In this situation the exact solution is available, which allows us to test the accuracy of the numerical method. It follows from Eq. (2.3) that the total field in the upper-half space is the transmitted wave, given explicitly by

$$u(x_1, x_2) = \frac{4}{3} e^{i2\pi x_2}.$$

It is a propagating wave, which propagates along the x_2-axis and is invariant with respect to the x_1-axis due to the normal incidence and the symmetric geometry of the problem. Table 1 lists the $L^2(\Omega)$ and $H^1(\Omega)$ errors and their convergence rate as functions of the mesh size h and number of nodes N_n. The results indicate the convergence order in $H^1(\Omega)$ norm is even better than the theoretical order one in this example. Fig. 2 shows the graphs of the real part and the imaginary part of the field. Here and in the following graphs the fields are drawn with $h = 0.05$.

Example 2 (*TE case*). Consider an incoming plane wave incident with $\theta = \pi/4$ from the lower-half space to the upper-half space, where there is no scatterer. The exact solution is also available and the total field in the upper-half space is again the transmitted wave, which can be analytically written as

$$u(x_1, x_2) = \frac{(4 - 2\sqrt{2}i)}{3} e^{i2\sqrt{2}\pi x_1} e^{-2\pi x_2}.$$

Table 1
$L^2(\Omega)$ and $H^1(\Omega)$ errors for Example 1.

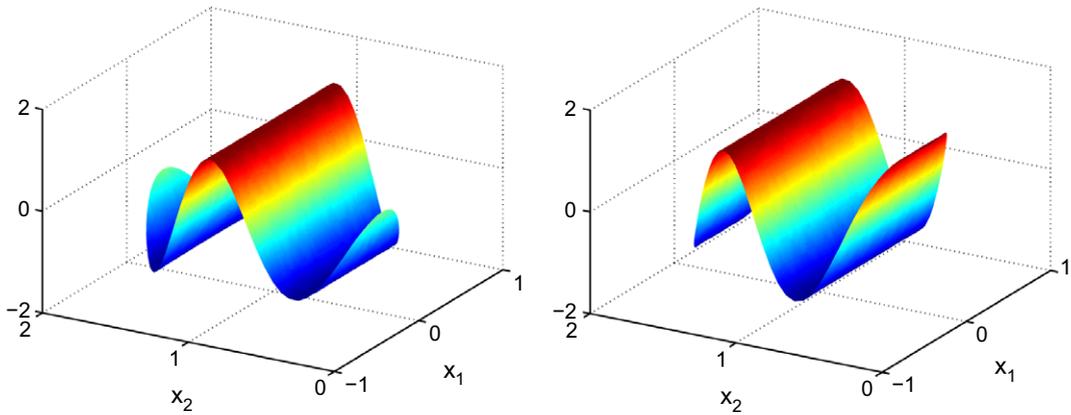| h_0	N_n	$\|u - u_h\|_{0,\Omega}$	Rate	$\|u - u_h\|_{1,\Omega}$	Rate
0.2	49	4.3698e−1		1.6830e−0	
0.1	203	1.1111e−1	1.98	4.5417e−1	1.89
0.05	808	2.6722e−2	2.01	1.5911e−1	1.51
0.025	3257	6.2727e−3	2.09	5.7641e−2	1.46
0.0125	13,046	1.5274e−3	2.04	1.9455e−2	1.57

Fig. 2. Numerical solution of Example 1 in TE case for $h = 0.05$. (Left) the real part of the transmitted field; (right) the imaginary part of the transmitted field.

As can be seen, the transmitted wave is an evanescent wave since the incident angle, $\pi/4$ is larger than the critical angle, $\pi/6$. The evanescent wave propagates in the x_1 direction but exponentially decays in the x_2 direction. Evanescent waves are crucial in near-field optical microscopy, which contribute to the super-resolving capability of near-field optics due to their high spatial frequency. Table 2 lists the $L^2(\Omega)$ and $H^1(\Omega)$ errors and their convergence rate as functions of the mesh size h and number of nodes N_n. The results indicate the rate of convergence for $H^1(\Omega)$ as predicted, order one, in this example. The real part and the imaginary part of the computed transmitted field are shown in Fig. 3.

Example 3 (*TE case*). Consider the same incident wave as in Example 1, i.e., normal incidence. Suppose there is a circular disc in the upper-half space, centered at $(0, 1)$ with radius 0.25. The disc is coated with a 0.25-thick lossy dielectric layer. The relative permittivity is defined as

$$\varepsilon_r = \begin{cases} 2.5 & \text{for } |\mathbf{x}| < 0.25, \\ 1.5 + i0.5 & \text{for } 0.25 < |\mathbf{x}| < 0.5, \\ 1.0 & \text{for } |\mathbf{x}| > 0.5. \end{cases}$$

Table 2
$L^2(\Omega)$ and $H^1(\Omega)$ errors for Example 2.

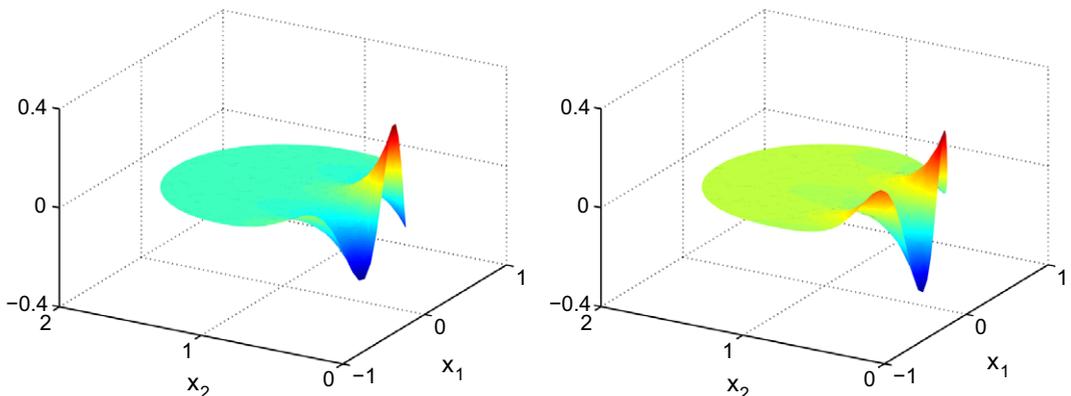| h	N_n	$\|u - u_h\|_{0,\Omega}$	Rate	$\|u - u_h\|_{1,\Omega}$	Rate
0.2	49	2.2203e−2		3.6733e−1	
0.1	203	4.2529e−3	2.38	1.6808e−1	1.12
0.05	808	8.1282e−4	2.39	7.5799e−2	1.15
0.025	3257	1.8054e−4	2.17	4.0166e−2	0.92
0.0125	13,046	3.7459e−5	2.27	2.0846e−2	0.95

Fig. 3. Numerical solution of Example 2 for $h = 0.05$. (Left) the real part of the scattered field; (right) the imaginary part of the scattered field.

In practice, the interested parameter is the radar cross section [29], which is defined by

$$\sigma = \frac{4}{\kappa_1}|P(\varpi)|^2,$$

where ϖ is the observation angle and P is the far-field coefficient given by

$$P(\varpi) = \int_\Gamma [\phi - i\kappa_1(\mathbf{n}_1\cos\varpi + \mathbf{n}_2\sin\varpi)u]e^{-i\kappa_1(x_1\cos\varpi + x_2\sin\varpi)}ds.$$

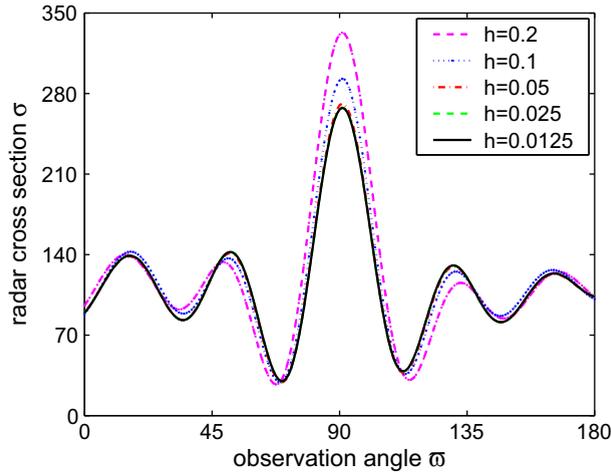**Fig. 4.** Radar cross section for Example 3 in TE case.

Table 3
H^1 errors for Example 4.

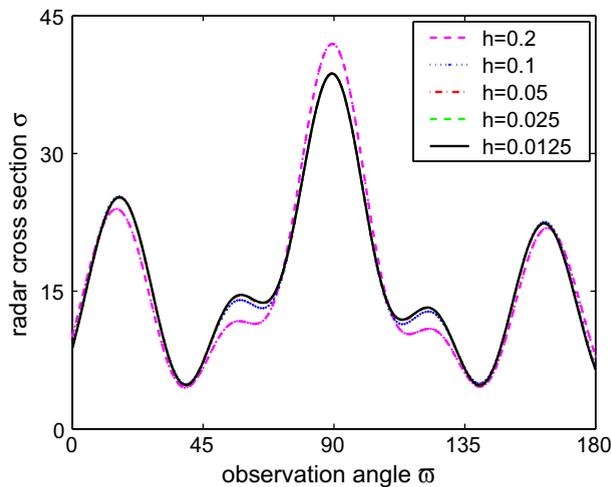| h	N_n	e_0	Rate	e_1	Rate	e_2	Rate
0.2	49	1.2481e−0		4.5086e−0		9.8347e−2	
0.1	203	4.8284e−1	1.37	2.0641e−0	1.12	4.6411e−2	1.08
0.05	808	2.1496e−1	1.17	9.6780e−1	1.09	2.1124e−2	1.14
0.025	3257	1.0365e−1	1.05	4.8773e−1	0.99	1.0851e−2	0.96
0.0125	13,046	4.8410e−2	1.10	2.2317e−1	1.13	4.9331e−3	1.14

Fig. 5. Radar cross section for Example 5 in TM case.

Here $\mathbf{n} = (\mathbf{n}_1, \mathbf{n}_2)$ is the unit outward normal to the boundary Γ. Fig. 4 shows the bistatic scattering patterns for the coated circular cylinder with different mesh sizes. Though there is no analytical solution for this example, from the graphs, one see a rather clear convergence pattern of the radar cross section and thus the numerical solutions.

Example 4 (*TM case*). To test the accuracy of the numerical method for the TM polarization, we consider the cases where the sample is not present. Let an incoming plane wave be incident from the lower-half space to the upper-half space with incident angle $\theta_i = i\pi/6$, $i = 0, 1, 2$. The total field in the upper-half space is the transmitted wave, which can be explicitly given from Eq. (2.3). Table 3 lists the $H^1(\Omega)$ errors, e_i, and their convergence rates as functions of the mesh size h and number of nodes N_n at different incident angle θ_i. It was proved in Theorem 3.1 that there exists a unique solution $u \in H^1(\Omega)$. Since there is no sample present and the medium is homogeneous in the computational domain, elliptic regularity theory may be applied to prove that $u \in H^2(\Omega)$ even for the TM case. The numerical results show the convergence order in $H^1(\Omega)$ norm verify the theoretical order one in this example.

Example 5 (*TM case*). This example has the same geometry configuration as that for Example 3. Therefore the exact solution is not available. Fig. 5 shows the bistatic scattering patterns for the coated circular disc with different mesh sizes. Once again, from the graphs, a rather clear convergence pattern can be seen for the radar cross section and thus for the numerical solutions.

6. Concluding remarks

A method of coupling of the finite element and boundary integral methods is developed for solving the electromagnetic scattering of an inhomogeneity embedded in a two-layered background medium for both the transverse electrical and magnetic polarization cases. The method is to enclose the inhomogeneous sample with a fictitious surface to separate the finite element region from the exterior region where the boundary integral equation applies. The field inside the surface is formulated using the finite element method, whereas those exterior to the surface can be expressed in terms of surface integrals. The interior and exterior are finally coupled via the field continuity conditions, leading to a complete system for the solution of interior and surface fields. The well-posedness of the continuous and discrete problems, as well as optimal error estimates for the coupled variational approximation, are established. A set of numerical examples are reported to illustrate the performance of the proposed method and show the basic features of wave propagation in layered medium. The numerical experiments indicate that the method is accurate and efficient.

Due to the complex geometry of the sample, e.g. the sample may consist of a thin coating, a sharp tip, an irregular surface or/and discontinuous dielectric permittivity, the solution may have singularities which slow down the convergence as using uniform mesh refinements and make uniform mesh refinements uneconomical. We are currently developing an adaptive coupling of finite element and boundary integral methods which will be more efficient for solving the electromagnetic scattering problem when having above-mentioned issues. We also intend to extend the method to more complicated three-dimensional Maxwell's equations, which obviously requires fast algorithms to speed up the evaluation of the boundary integrals. The algorithms and computational results will be reported elsewhere.

Acknowledgment

Appendix A. Fundamental solutions

We shall first introduce the fundamental solution of the two-dimensional Helmholtz equation in a two-layered medium for the transverse electric polarization case, then followed by the case of transverse magnetic polarization.

A.1. TE polarization

For the observation point $\mathbf{x} = (x_1, x_2)$ and source point $\mathbf{y} = (y_1, y_2)$, the fundamental solution of Helmholtz equation in a two-layered background medium in $\mathbb{R}^2$ satisfies

$$\Delta G_{\mathrm{TE}}(\mathbf{x}, \mathbf{y}) + \kappa_b^2(\mathbf{x}) G_{\mathrm{TE}}(\mathbf{x}, \mathbf{y}) = -\delta(\mathbf{x} - \mathbf{y}), \tag{A.1}$$

with jump conditions

$$G_{\mathrm{TE}}(\mathbf{x}, \mathbf{y})|_{x_2=0^+} = G_{\mathrm{TE}}(\mathbf{x}, \mathbf{y})|_{x_2=0^-},$$
$$\left. \frac{\partial G_{\mathrm{TE}}(\mathbf{x}, \mathbf{y})}{\partial x_2} \right|_{x_2=0^+} = \left. \frac{\partial G_{\mathrm{TE}}(\mathbf{x}, \mathbf{y})}{\partial x_2} \right|_{x_2=0^-}, \tag{A.2}$$

where the wavenumber

$$\kappa_b(\mathbf{x}) = \begin{cases} \kappa_1 & \text{for } x_2 > 0, \\ \kappa_2 & \text{for } x_2 < 0. \end{cases}$$

Define

$$\beta_i = \begin{cases} \sqrt{\kappa_i^2 - \xi^2} & \text{for } |k_i| > |\xi|, \\ i\sqrt{\xi^2 - \kappa_i^2} & \text{for } |k_i| < |\xi|, \end{cases}$$

it follows from the Fourier transform that the fundamental solution is given by

- $x_2 > 0$, $y_2 > 0$

  $$G_{\text{TE}}(\mathbf{x}, \mathbf{y}) = \Psi_{\text{TE}}^{(1)}(\mathbf{x}, \mathbf{y}) + \Phi_1(\mathbf{x}, \mathbf{y}),$$

- $x_2 < 0$, $y_2 < 0$

  $$G_{\text{TE}}(\mathbf{x}, \mathbf{y}) = \Psi_{\text{TE}}^{(2)}(\mathbf{x}, \mathbf{y}) + \Phi_2(\mathbf{x}, \mathbf{y}),$$

- $x_2 > 0$, $y_2 < 0$

  $$G_{\text{TE}}(\mathbf{x}, \mathbf{y}) = \Psi_{\text{TE}}^{(3)}(\mathbf{x}, \mathbf{y}),$$

- $x_2 < 0$, $y_2 > 0$

  $$G_{\text{TE}}(\mathbf{x}, \mathbf{y}) = \Psi_{\text{TE}}^{(4)}(\mathbf{x}, \mathbf{y}),$$

where

$$\Psi_{\text{TE}}^{(1)}(\mathbf{x}, \mathbf{y}) = \frac{i}{4\pi} \int_{-\infty}^{\infty} \frac{1}{\beta_1} \frac{\beta_1 - \beta_2}{\beta_1 + \beta_2} e^{i\beta_1(x_2 + y_2)} e^{i\xi(x_1 - y_1)} d\xi, \tag{A.3}$$

$$\Psi_{\text{TE}}^{(2)}(\mathbf{x}, \mathbf{y}) = \frac{i}{4\pi} \int_{-\infty}^{\infty} \frac{1}{\beta_2} \frac{\beta_2 - \beta_1}{\beta_1 + \beta_2} e^{-i\beta_2(x_2 + y_2)} e^{i\xi(x_1 - y_1)} d\xi, \tag{A.4}$$

$$\Psi_{\text{TE}}^{(3)}(\mathbf{x}, \mathbf{y}) = \frac{i}{2\pi} \int_{-\infty}^{\infty} \frac{e^{i(\beta_1 x_2 - \beta_2 y_2)}}{\beta_1 + \beta_2} e^{i\xi(x_1 - y_1)} d\xi, \tag{A.5}$$

$$\Psi_{\text{TE}}^{(4)}(\mathbf{x}, \mathbf{y}) = \frac{i}{2\pi} \int_{-\infty}^{\infty} \frac{e^{i(\beta_1 y_2 - \beta_2 x_2)}}{\beta_1 + \beta_2} e^{i\xi(x_1 - y_1)} d\xi, \tag{A.6}$$

and Φ_i is the fundamental solution of the Helmholtz equation in homogeneous background medium in $\mathbb{R}^2$ with wavenumber κ_i, i.e.,

$$\Phi_i(\mathbf{x}, \mathbf{y}) = \frac{i}{4} H_0^{(1)}(\kappa_i |\mathbf{x} - \mathbf{y}|), \quad i = 1, 2.$$

Here $H_0^{(1)}$ is the Hankel function of the first kind with order zero. Applying the dominated convergence theorem to (A.3)–(A.6) and their derivatives, it is easy to see that $\Psi_{\text{TE}}^{(j)} \in C^\infty(\mathbb{R}^2 \times \mathbb{R}^2 \setminus \{0\} \times \{0\})$, $j = 1, \ldots, 4$.

A.2. TM polarization

For the observation point $\mathbf{x} = (x_1, x_2)$ and source point $\mathbf{y} = (y_1, y_2)$, the fundamental solution of Helmholtz equation in the two-layered background medium in $\mathbb{R}^2$ satisfies

$$\nabla \cdot \left(\kappa_b^{-2}(\mathbf{x}) \nabla G_{\text{TM}}(\mathbf{x}, \mathbf{y}) \right) + G_{\text{TM}}(\mathbf{x}, \mathbf{y}) = -\delta(\mathbf{x} - \mathbf{y}), \tag{A.7}$$

with jump conditions

$$\begin{aligned} G_{\text{TM}}(\mathbf{x}, \mathbf{y})\big|_{x_2 = 0^+} &= G_{\text{TM}}(\mathbf{x}, \mathbf{y})\big|_{x_2 = 0^-}, \\ \frac{1}{\kappa_1^2} \frac{\partial G_{\text{TM}}(\mathbf{x}, \mathbf{y})}{\partial x_2}\bigg|_{x_2 = 0^+} &= \frac{1}{\kappa_2^2} \frac{\partial G_{\text{TM}}(\mathbf{x}, \mathbf{y})}{\partial x_2}\bigg|_{x_2 = 0^-}. \end{aligned} \tag{A.8}$$

Similarly, it follows from the Fourier transform and the integral representation of the Hankel function that the fundamental solution in TM case is given by

- $x_2 > 0$, $y_2 > 0$

  $$G_{\text{TE}}(\mathbf{x}, \mathbf{y}) = \Psi_{\text{TM}}^{(1)}(\mathbf{x}, \mathbf{y}) + \Phi_1(\mathbf{x}, \mathbf{y}),$$

- $x_2 < 0$, $y_2 < 0$

$$G_{\text{TE}}(\mathbf{x}, \mathbf{y}) = \Psi_{\text{TM}}^{(2)}(\mathbf{x}, \mathbf{y}) + \Phi_2(\mathbf{x}, \mathbf{y}),$$

- $x_2 > 0, \ y_2 < 0$

$$G_{\text{TE}}(\mathbf{x}, \mathbf{y}) = \Psi_{\text{TM}}^{(3)}(\mathbf{x}, \mathbf{y}),$$

- $x_2 < 0, \ y_2 > 0$

$$G_{\text{TE}}(\mathbf{x}, \mathbf{y}) = \Psi_{\text{TM}}^{(4)}(\mathbf{x}, \mathbf{y}),$$

where

$$\Psi_{\text{TM}}^{(1)}(\mathbf{x}, \mathbf{y}) = \frac{i}{4\pi} \int_{-\infty}^{\infty} \frac{1}{\beta_1} \frac{\beta_1 \kappa_2^2 - \beta_2 \kappa_1^2}{\beta_1 \kappa_2^2 + \beta_2 \kappa_1^2} e^{i\beta_1(x_2+y_2)} e^{i\xi(x_1-y_1)} d\xi, \tag{A.9}$$

$$\Psi_{\text{TM}}^{(2)}(\mathbf{x}, \mathbf{y}) = \frac{i}{4\pi} \int_{-\infty}^{\infty} \frac{1}{\beta_2} \frac{\beta_2 \kappa_1^2 - \beta_1 \kappa_2^2}{\beta_1 \kappa_1^2 + \beta_2 \kappa_1^2} e^{-i\beta_2(x_2+y_2)} e^{i\xi(x_1-y_1)} d\xi, \tag{A.10}$$

$$\Psi_{\text{TM}}^{(3)}(\mathbf{x}, \mathbf{y}) = \frac{i}{2\pi} \int_{-\infty}^{\infty} \frac{\kappa_2^2}{\beta_1 \kappa_2^2 + \beta_2 \kappa_1^2} e^{i(\beta_1 x_2 - \beta_2 y_2)} e^{i\xi(x_1-y_1)} d\xi, \tag{A.11}$$

$$\Psi_{\text{TM}}^{(4)}(\mathbf{x}, \mathbf{y}) = \frac{i}{2\pi} \int_{-\infty}^{\infty} \frac{\kappa_1^2}{\beta_1 \kappa_2^2 + \beta_2 \kappa_1^2} e^{i(\beta_1 y_2 - \beta_2 x_2)} e^{i\xi(x_1-y_1)} d\xi. \tag{A.12}$$

References

[1] H. Ammari, G. Bao, Coupling of finite element and boundary element methods for the scattering by periodic chiral structures, J. Comput. Math. 26 (2008) 261–283.
[2] H. Ammari, J.-C. Nédélec, Couplage élements finis-équation intégrale pour les équations de Maxwell hétérogène, Equations aux Dérivées Partielles et Applications, Articles Dédiées à J.-L. Lions, Elsevier, 1998, pp. 19–34.
[3] H. Ammari, J.-C. Nédélec, Coupling of finite and boundary element methods for the time-harmonic Maxwell equations. Part II: a symmetric formulation, in: Rossmann et al. (Eds.), Operator Theory: Advances and Applications 108, The Maz'ya Anniversary Collection, vol. 101, 1999, pp. 23–32.
[4] H. Ammari, J.-C. Nédélec, Coupling integral equations method and finite volume elements for the resolution of the Leontovich boundary value problem for the time-harmonic Maxwell equations in three dimensional heteregeneous media, in: Mathematical Aspects of Boundary Element Methods, Research Notes in Mathematics, vol. 414, 1999, pp. 11–22.
[5] G. Bao, Finite element approximation of time harmonic waves in periodic structures, SIAM J. Numer. Anal. 32 (1995) 1155–1169.
[6] G. Bao, P. Li, Inverse medium scattering problems in near-field optics, J. Comput. Math. 25 (2007) 252–265.
[7] J. Bérenger, A perfectly matched layer for the absorbtion of electromagnetic waves, J. Comput. Phys. 114 (1994) 110–117.
[8] S. Brenner, L. Scott, The Mathematical Theory of Finite Element Methods, Springer-Verlag, New York, 1994.
[9] F. Brezzi, C. Johnson, On the coupling of boundary integral and finite element methods, Calcolo 16 (1979) 189–201.
[10] S.N. Chandler-Wilde, B. Zhang, Electromagnetic scattering by an inhomogeneous conducting or dielectric layer on a perfectly conducting plate, Proc. Roy. Soc. Lond. Ser. A 454 (1998) 519–542.
[11] G. Chen, J. Zhou, Boundary Element Methods, Academic Press, London, 1992.
[12] D. Colton, R. Kress, Integral Equation Methods in Scattering Theory, Wiley, New York, 1983.
[13] D. Colton, R. Kress, Inverse Acoustic and Electromagnetic Scattering Theory, second ed., Springer-Verlag, Berlin, 1998.
[14] M. Costabel, E.P. Stephan, Coupling of finite and boundary element methods for an elastoplastic interface problem, SIAM J. Numer. Anal. 27 (1990) 1212–1226.
[15] P. Carney, J. Schotland, Near-field tomography, in: G. Uhlmann (Ed.), Inside Out: Inverse Problems and Applications, Cambridge University Press, 2003, pp. 133–168.
[16] D. Courjon, Near-field Microscopy and Near-field Optics, Imperial College Press, London, 2003.
[17] J. Coyle, Locating the support of objects contained in a two-layered background medium in two dimensions, Inverse Probl. 16 (2000) 275–292.
[18] P.-M. Cutzach, C. Hazard, Existence, uniqueness and analyticity properties for electromagnetic scattering in a two-layered medium, Math. Meth. Appl. Sci. 21 (1998) 433–461.
[19] M. Durán, I. Muga, J.-C. Nédélec, The Helmholtz equation with impedance in a half-plane, C.R. Acad. Sci. Paris Ser. I 340 (2005) 483–488.
[20] J. Elschner, G. Schmidt, Diffraction in periodic structures and optimal design of binary gratings. I. Direct problem and gradient formulas, Math. Meth. Appl. Sci. 21 (1998) 1297–1342.
[21] B. Engquist, A. Majda, Absorbing boundary conditions for the numerical simulation of waves, Math. Comput. 31 (1977) 629–651.
[22] R. Freund, N. Nachtigal, An implementation of the QMR method based on coupled two-term recurrences, SIAM J. Sci. Comput. 15 (1994) 313–337.
[23] G.N. Gatica, G.C. Hisao, On the coupled BEM and FEM for a nonlinear exterior Dirichlet problem in $\mathbb{R}^2$, Numer. Math. 61 (1992) 171–214.
[24] G.N. Gatica, W.L. Wendland, Coupling of mixed finite elements and boundary elements for linear and nonlinear elliptic problems, Appl. Anal. 63 (1996) 39–75.
[25] D. Givoli, J. Keller, Exact non-reflecting boundary conditions, J. Comput. Phys. 82 (1989) 172–192.
[26] T. Hagstrom, Radiation boundary conditions for the numerical simulation of waves, Acta Numer. 8 (1999) 47–106.
[27] R. Higdon, Absorbing boundary conditions for acoustic and elastic waves in stratified media, J. Comput. Phys. 101 (1992) 386–418.
[28] G.C. Hsiao, The coupling of boundary element and finite element methods, Math. Mech. 6 (1990) 493–503.
[29] J. Jin, The Finite Element Method in Electromagnetics, Wiley, New York, 1993.
[30] C. Johnson, J.-C. Nédélec, On the coupling of boundary integral and finite element methods, Math. Comput. 35 (1980) 1063–1079.
[31] A. Kirsch, P. Monk, Convergence analysis of the coupled finite element method and spectral method in acoustic scattering, IMA J. Numer. Anal. 9 (1990) 425–447.
[32] G. Kristensson, Uniqueness theorem for Helmholtz equation: penetrable media with an infinite interface, SIAM J. Math. Anal. 11 (1980) 1104–1116.
[33] P. Li, Numerical simulations of global approach for photon scanning tunneling microscopy: coupling of finite-element and boundary integral methods, J. Opt. Soc. Am. A 25 (2008) 1929–1936.
[34] W. McLean, Strongly Elliptic Systems and Boundary Integral Equations, Cambridge University Press, Cambridge, 2000.
[35] S. Meddahi, A. Márquez, V. Selgas, Computing acoustic waves in an inhomogeneous medium of the plane by a coupling of spectral and finite elements, SIAM J. Numer. Anal. 41 (2003) 1729–1750.

[36] P. Monk, Finite Element Methods for Maxwell's Equations, Oxford University Press, Oxford, UK, 2003.
[37] J.-C. Nédélec, Acoustic and Electromagnetic Equations: Integral Representations for Harmonic Problems, Springer, New York, 2000.
[38] P. Persson, G. Strang, A simple mesh generator in Matlab, SIAM Rev. 46 (2004) 329–345.
[39] T. Tran, The *K*-operator and the Galerkin method for strongly elliptic equations on smooth curves: local estimates, Math. Comput. 64 (1995) 501–513.
[40] E. Turkel, A. Yefet, Absorbing PML boundary layers for wave-like equations, Appl. Numer. Math. 27 (1998) 533–557.
[41] T. Van, A.W. Wood, Finite element analysis of electromagnetic scattering from a cavity, IEEE Trans. Antennas Propag. 51 (2003) 130–137.
[42] Y. Xu, Radiation condition and scattering problem for the time-harmonic acoustic waves in a stratified medium with a nonstratified inhomogeneity, IMA J. Appl. Math. 54 (1995) 9–29.
[43] D.-H. Yu, Natural Boundary Integral Method and Its Applications, Science Press, Kluwer Academic Publishers, 2002.
[44] B. Zhang, S.N. Chandler-Wilde, Acoustic scattering by an inhomogeneous layer on a rigid plate, SIAM J. Appl. Math. 58 (1998) 1931–1950.